Phosphoproteomic analysis of the antitumor effects of ginsenoside Rg3 in human breast cancer cells

MINGJIN ZOU[1], JING WANG[2], JIDONG GAO[2], HUI HAN[3*] and YI FANG[2*]

[1]Department of Clinical Laboratory, Qilu Hospital of Shandong University, Jinan, Shandong 250012; [2]Department of Breast Surgical Oncology, National Cancer Center and Cancer Hospital, Chinese Academy of Medical Sciences and Peking Union Medical College, Beijing 100021; [3]Department of Infection Control, Qilu Hospital of Shandong University, Jinan, Shandong 250012, P.R. China

Received December 13, 2016; Accepted November 10, 2017

DOI: 10.3892/ol.2017.7654

Abstract. The incidence of breast cancer has been increasing in China and the age of breast cancer onset is earlier compared with Western countries. Compounds commonly used in Traditional Chinese Medicine (TCM) are an important source of anticancer drugs. Ginseng is one of the most common medicines used in TCM. Ginsenosides, which are saponins found in the ginseng plant, are the major active components responsible for the chemopreventive effects of ginseng in cancer. However, the mechanisms by which ginsenosides exert their anticancer effects remain elusive. The current study combined tandem mass tag (TMT)-based quantification with titanium dioxide-based phosphopeptide enrichment to quantitatively analyze the changes in phosphoproteomes in breast cancer MDA-MB-231 cells that occur following treatment with the ginsenoside Rg3. A total of 5,140 phosphorylation sites on 2,041 phosphoproteins were quantified and it was demonstrated that the phosphorylation status of 13 sites were altered in MDA-MB-231 cells following treatment with Rg3. The perturbed phosphoproteins were: Cleavage and polyadenylation specificity factor subunit 7, elongation factor 2 (EEF2), HIRA-interacting protein 3, melanoma-associated antigen D2, myosin phosphatase Rho-interacting protein, probable E3 ubiquitin-protein ligase MYCBP2, PRKC apoptosis WT1 regulator protein, protein phosphatase 1 regulatory subunit 12A, E3 SUMO-protein ligase RanBP2, Septin-9, thymopoietin, and E3 UFM1-protein ligase 1. Western blotting confirmed that Rg3 increased the phosphorylation of EEF2 on Thr57 but did not alter the protein expression of EEF2 in MDA-MB-231 and HCC1143 cells. These ginsenoside Rg3-regulated proteins are involved in various biological processes, including protein synthesis, cell division and the inhibition of nuclear factor-κB signaling. The results of the present study revealed that Rg3 exerts its anticancer effects via a combination of different signaling pathways.

Correspondence to: Dr Yi Fang, Department of Breast Surgical Oncology, National Cancer Center and Cancer Hospital, Chinese Academy of Medical Sciences and Peking Union Medical College, 17 Panjiayuan Nanli, Chaoyangqu, Beijing 100021, P.R. China
E-mail: fangyi@cicams.ac.cn

Dr Hui Han, Department of Infection Control, Qilu Hospital of Shandong University, 107 Wenhua West Road, Jinan, Shandong 250012, P.R. China
E-mail: hanhui.sdu@gmail.com

*Contributed equally

Abbreviations: TMT, tandem mass tag; EEF2, elongation factor 2

Key words: ginsenoside Rg3, tandem mass tag, quantitative phosphoproteomics, elongation factor 2

Introduction

Breast cancer is the most common cancer and the sixth leading cause of cancer-associated mortality in Chinese women (1). The overall incidence of breast cancer has been increasing in China and the age of onset is earlier compared with Western countries; in China, breast cancer incidence peaks at the age of 50 (2). Plant-derived active constituents, which are frequently used in Traditional Chinese Medicine (TCM), as well as their semi-synthetic or synthetic analogs, are a major source of anticancer drugs. Ginseng, including American ginseng (*Panax quinquefolius* L.) and Asian ginseng (*Panax ginseng* C.A. Meyer) is the root of *Panax* plant (which belongs to the Araliaceae family) and is one of the most common compounds used in TCM (3-5). Ginsenosides, which are saponins found in ginseng, are the major active components responsible for their chemopreventive effects against cancer (6).

Ginsenoside Rg3, which is extracted from the steamed *Panax ginseng* C.A. Meyer, exhibits anticancer properties. Chen *et al* (7) demonstrated that Rg3 decreases the metastasis of breast cancer cells and the expression of C-X-C chemokine receptor type 4, which serves an important role in metastasis. Kim *et al* (8) determined that Rg3 induces apoptosis in MDA-MB-231 cells via classical mitochondria-dependent caspase activation. Furthermore, it was indicated that Rg3 induces apoptosis by blocking nuclear factor (NF)-κB signaling via inactivation of extracellular regulated kinase (ERK) and protein kinase B (Akt) and destabilization of mutant p53 (9).

Improving understanding of the mechanisms by which Rg3 executes its anticancer functions may aid the development of novel therapies to treat breast cancer.

Multiplexed quantification has been used to analyze complex signaling pathways. This is performed with the use of isobaric labeling reagents, including tandem mass tags (TMT) (10) and isobaric tags for relative and absolute quantification (iTRAQ) (11), combined with phosphopeptide enrichment and mass spectrometry (MS). Nirujogi *et al* (12) used an 8-plex TMT labeling strategy with titanium dioxide (TiO_2)-based phosphopeptide enrichment to assess changes of the phosphoproteome in the brains of rats following exposure to the nerve agent VX. Roitinger *et al* (13) combined a 4-plex iTRAQ labeling strategy with a phosphopeptide enrichment pipeline (immobilized metal affinity chromatography coupled with metal oxide affinity chromatography) to characterize the DNA damage response signaling pathway in *Arabidopsis thaliana*. Furthermore, a previous study by the current authors combined a 6-plex TMT labeling method with TiO_2-based phosphopeptide enrichment to evaluate the short-term effects of genistein on the phosphorylation-mediated signal transduction pathway in MDA-MB-231 cells. The results revealed that genistein modulated the cell cycle and the DNA damage response pathway (14). In the current study, a TMT-based quantitative phosphoproteomics approach was used to identify Rg3-regulated proteins in breast cancer MDA-MB-231 cells following short-term treatment. A total of 5,907 phosphorylation sites on 2,143 phosphoproteins were identified out of 3,597 proteins. Out of these phosphorylation sites, 5,140 were quantified. The results demonstrated that 13 were altered in MDA-MB-231 cells following Rg3 treatment. The phosphoproteins regulated by Rg3 are involved in protein synthesis, cell division and NF-κB signaling inhibition. The results of the current study therefore suggest that the anticancer effects of Rg3 are dependent on various mechanisms in breast cancer cells.

Materials and methods

Cell lines and reagents. The breast cancer cell line MDA-MB-231 was maintained in Dulbecco's Modified Eagle's medium (DMEM) supplemented with 10% fetal bovine serum (FBS), 29.2 μg/ml L-glutamine, 100 units/ml of penicillin and 100 μg/ml of streptomycin (all Thermo Fisher Scientific, Inc., Waltham, MA, USA) at 37˚C in 5% CO_2. The breast cancer cell line HCC1143 was maintained in RPMI-1640 supplemented with 10% FBS, 29.2 μg/ml of L-glutamine, 100 units/ml of penicillin and 100 μg/ml of streptomycin at 37˚C in 5% CO_2. The cell lines were purchased from the American Type Culture Collection (Manassas, VA, USA). Ginsenoside Rg3 and antibodies against GAPDH (G8795, mouse monoclonal), elongation factor 2 (EEF2) (SAB5300110, mouse monoclonal) and phosphorylated (p)-EEF2 (Thr57) (SAB4503817, rabbit polyclonal) were purchased from Sigma-Aldrich; Merck KGaA (Darmstadt, Germany). The secondary Amersham ECL HRP conjugated antibodies against rabbit IgG (NA934V) and mouse IgG (NA931V), nitrocellulose membrane and Amersham ECL Western Blotting Detection Reagents were purchased from GE Healthcare Life Sciences (Pittsburgh, PA, USA). TiO_2 nanobeads (5 μm beads) were purchased from GL Sciences Inc. (Torrance, CA, USA). Trypsin (Tosyl phenylalanyl chloromethyl ketone-treated) was purchased from Worthington Biochemical Corp. (Lakewood, NJ, USA). DMEM, RPMI-1640, Penicillin-Streptomycin-Glutamine (100X), the halt™ Protease and Phosphatase Inhibitor Cocktail (100X), TMTsixplex™ Isobaric Label Reagent Set and all other chemicals were purchased from Thermo Fisher Scientific, Inc. (Waltham, MA, USA).

Cell lysis, protein digestion and TMT labeling. Exponentially growing MDA-MB-231 cells were plated at $3x10^6$ cells per 150 mm plate overnight. Three populations of cells were treated with 40 μM ginsenoside Rg3 for 0, 3 or 24 h. Experiments were performed in duplicate. Cell lysis and protein extraction were performed as previously described (14). Briefly, following treatment, cells were washed with PBS and lysed in lysis buffer [4% SDS, 50 mM triethylammonium bicarbonate (TEABC), 10 mM sodium fluoride, 1 mM sodium orthovanadate, 1 mM β-glycerophosphate and 2.5 mM sodium pyrophosphate] via sonication at 4˚C for 4 min at 10 sec/pulse and a frequency of 0.05 Hz. Following centrifugation at 16,000 x g at 20˚C for 15 min, the supernatant was collected and protein concentration was determined using a Pierce™ Bicinchoninic acid assay (Thermo Scientific, Inc.). An equal amount of protein (400 μg) from each group of cells was reduced by dithiothreitol at a final concentration of 5 mM at 60˚C for 20 min and alkylated using 10 mM iodoacetamide for 10 min at 25˚C in the dark.

Samples were then subjected to the filter-assisted sample preparation (FASP) protocol (15) with minor modifications (14). Processed samples were subsequently transferred to a fresh tube and subjected to tryptic digestion overnight at 37˚C. The resulting peptides were dried completely in a vacuum concentrator and stored at -80˚C. TMT labeling was performed following the manufacturer's protocol in the TMTsixplex™ Isobaric Label Reagent Set. Briefly, tryptic peptides from each sample was reconstituted in 100 μl of 50 mM TEABC buffer and mixed with the TMT reagent reconstituted in 41 μl anhydrous acetonitrile (ACN) and incubated at 25˚C for 1 h. All labeled peptides from each sample were mixed, completely dried in a vacuum concentrator and stored at -80˚C.

Fractionation of peptides by basic reversed phase high-performance liquid chromatography (bRP-HPLC). The peptide mixture was fractionated on an Agilent 1100 Series HPLC system (Agilent Technologies, Inc., Santa Clara, CA, USA) using basic reversed-phase chromatography at a flow rate of 400 μl/min. The TMT-labeled peptide mixture was resuspended in 1 ml of 10 mM TEABC (pH 8.0) and loaded on an XBridge BEH C18 Column (130 Å, 5 μm, 4.6x250 mm; Waters, Milford, MA). The mobile phase consisted of 10 mM TEABC, pH 8.0 (buffer A) and 10 mM TEABC, 90% acetonitrile, pH 8.0 (buffer B). The sample was loaded was onto the column and peptides were subsequently separated using the following gradient: 2 min isocratic hold at 0% B, 0-15% solvent B in 8 min; 15-28.5% solvent B in 33 min; 28.5-34% solvent B in 5.5 min; 34-60% solvent B in 13 min, for a total gradient time of 64.5 min. Fractions were collected on a 96-well plate through the elution profile of the separation. A total of 5% of the collections from each well were merged

into 6 fractions and dried using vacuum centrifugation prior to proteomic analysis by liquid chromatography tandem mass spectrometry (LC-MS/MS). The remaining fractions from each well were merged into 12 fractions and dried using vacuum centrifugation for TiO_2-based phosphopeptide enrichment.

TiO_2-based phosphopeptide enrichment. The 12 fractions from bRP-HPLC were subjected to TiO_2-based phosphopeptide enrichment as described by Larsen *et al* (16), with minor modifications (14). Briefly, TiO_2 nanobeads were incubated with 2,5-dihydroxybenzoic acid (DHB) solution [80% v/v ACN, 3% v/v trifluoroacetic acid (TFA), 5% w/v DHB] for 20 min at 25˚C. Each fraction was resuspended in DHB solution and incubated with DHB-bound TiO_2 nanobeads [Peptides (mg): TiO_2 (mg)=1:1]. Phosphopeptide-bound TiO_2 nanobeads were washed twice with 400 μl washing solution (80% v/v ACN, 3% v/v TFA). Phosphopeptides were eluted three times with 20 μl 4% v/v ammonia into 20 μl 20% v/v TFA and dried completely using vacuum centrifugation. Dried phosphopeptides were resuspended in 50 μl 0.15% TFA and desalted using C18 Stage-Tips, made according to the protocol outlined by Rappsilber *et al* (17), prior to LC-MS/MS.

LC-MS/MS. LC-MS/MS analysis of peptides and phosphopeptides was performed using a reversed phase liquid chromatography Dionex chromatography system interfaced with a linear trap quadrupole-Orbitrap Velos mass spectrometer (Thermo Fisher Scientific, Inc.). Mass spectra of precursor and product ions were acquired in a high-resolution Orbitrap analyzer (Thermo Fisher Scientific, Inc.). Peptides were loaded onto an analytical column (10 cmx75 μm, Magic C18 AQ 5 μm, 120 Å; Thermo Fisher Scientific, Inc) by 0.1% v/v formic acid and eluted using an ACN gradient (0-60% v/v) containing 0.1% v/v formic acid. The settings were: i) Precursor scans (fourier transform mass spectrometry, FTMS) from 350-1,800 m/z at 30,000 resolution; and ii) MS2 scan (FTMS) of higher-energy collisional dissociation (HCD) fragmentation of the 10 most intense ions (isolation width, 1.20 m/z; normalized collision energy, 40.0; activation time, 0.1 ms; fourier transform (FT) first mass value, 110.00 (fixed) at a resolution of 15,000.

MS data analysis. Tandem mass spectra were searched using the Andromeda algorithm (18) against a human UniProt database (launched in February 2014, www.uniprot.org) using the MaxQuant platform (version 1.4.1.2, developed by Computational Systems Biochemistry; The Max Planck Institute, Munich, Germany). The search parameters included: 6-plex TMT, ≤2 missed cleavages, fixed modification (carbamidomethylation of cysteine residues), variable modification, (protein N-term acetylation), oxidation of methionine residues and phosphorylation of serine, threonine and tyrosine residues. The first and primary searches for monoisotopic peptide tolerance were set to 20 and 4.5 ppm, respectively. The MS/MS tolerance was set to 50 ppm. The maximum modifications per peptide were set to 5 and the maximum charge was set at 7. The reward type of the target-decoy analysis was selected. The peptide-spectrum match (PSM) false discovery rate (FDR), protein FDR and the site decoy fraction were set to 0.01. The minimum peptide length was set to 7. The minimal scores for unmodified and modified peptides were 0 and 40, respectively. The minimal δ scores for unmodified and modified peptides were 0 and 17, respectively. The minimum of unique and razor peptides for identification was set to 1. The reporter ion intensities for each PSM with a precursor ion fraction (PIF) >0.75 were calculated using MaxQuant. The quantification of identified proteins was determined by normalized reporter ion intensities using ≥1 razor/unique non-phosphopeptide. The quantification of each identified phosphosite was determined using the least modified peptide and normalized to produce normalized reporter ion intensities. The probability of phosphorylation of each Ser/Thr/Tyr site on each peptide was calculated using Andromeda software (also developed by Computational Systems Biochemistry, The Max Planck Institute, Munich, Germany) incorporated into the MaxQuant platform. MS proteomics data were deposited to the ProteomeXchange Consortium (19) via the proteomics identifications (PRIDE) partner repository and have the dataset identifier PXD003092.

Bioinformatics analysis. The molecular function and cellular localization of phosphoproteins were obtained using the protein annotation through evolutionary relationship (PANTHER) classification system (20,21). A literature search was carried out by searching the gene names of the Rg-3-regulated proteins against the PubMed database (http://www.pubmed.gov). The search results from the PubMed database were reviewed to identify the potential roles of these proteins in cancer-related signaling pathways.

Western blotting. MDA-MB-231 and HCC1143 cells were treated with ginsenoside Rg3 for 0, 3 and 24 h. The expression of the proteins EEF2 and p-EEF2 (Thr57) from each sample were analyzed by Western blotting to validate the significance of the proteomic results. Cells were lysed in modified radioimmunoprecipitation assay (RIPA) lysis buffer (50 mM Tris-HCl, pH 7.4, 150 mM NaCl, 1 mM EDTA, 1% Nonidet P-40, 0.25% sodium deoxycholate and 1X Halt™ Protease and Phosphatase Inhibitor Cocktail) followed by centrifugation at 16,000 x g at 4˚C for 20 min. The protein concentration of the supernatant was measured using a Pierce™ BCA Protein Assay kit (Thermo Fisher Scientific, Inc.), 50 μg was loaded into NuPAGE 4-12% Bis-Tris Protein Gels (Thermo Fisher Scientific, Inc.). Proteins were transferred onto nitrocellulose membranes (GE Healthcare Life Sciences). After blocking with 5% non-fat dry milk in PBS-T buffer at 4˚C for 4 h, the membranes were incubated in PBS-T buffer with the antibody against GAPDH (dilution, 1:10,000) as the loading control or the phosphospecific antibody against p-EEF2 (Thr57; dilution, 1:1,000) or anti-EEF2 antibody (dilution, 1:500) at 4˚C for overnight. Following 3 washes in PBS-T, the membranes were incubated with the corresponding HRP-conjugated secondary antibodies against mouse IgG (1:5,000) or rabbit IgG (1:10,000) at room temperature for 1 h. All films were developed with ECL reagents.

Results and Discussion

MS analysis of ginsenoside Rg3-treated MDA-MB-231 cells. Kim *et al* previously demonstrated that ginsenoside Rg3

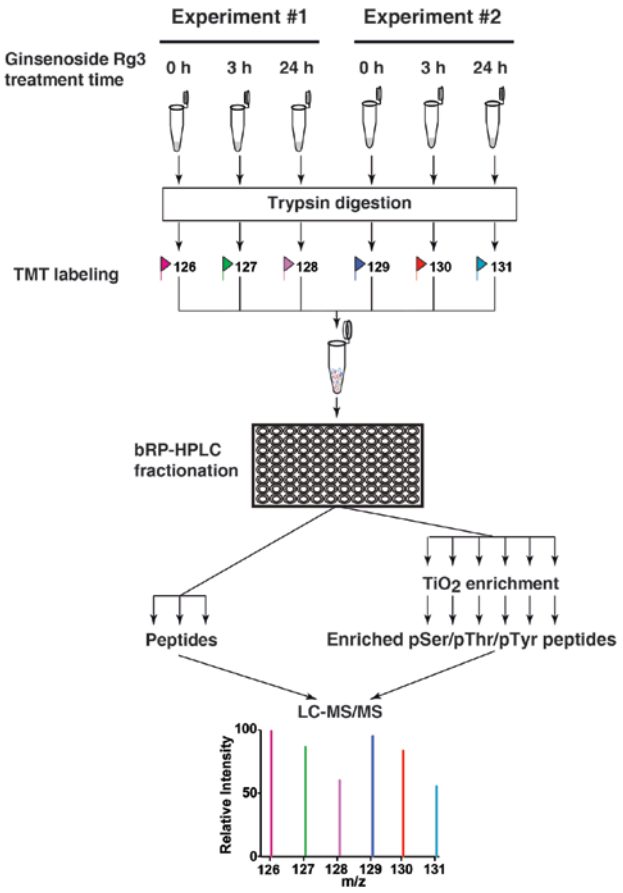

Figure 1. Schematic illustration of the TMT-based quantitative whole proteomic/phosphoproteomic pipeline. Cells treated with ginsenoside Rg3 for different time were subjected to filter-assisted sample preparation-based sample preparation. 6-plex TMT labeling and bRP-HPLC were performed and collected fractions were concatenated. A proportion of these fractions were subjected to TiO_2 enrichment. Enriched phosphopeptides, along with unprocessed peptides were analyzed using an Orbitrap-equipped mass spectrometer. TMT, tandem mass tag; LC-MS/MS, liquid chromatography tandem mass spectrometry; bRP-HPLC, basic reversed phase high-performance liquid chromatography; TiO_2, titanium dioxide.

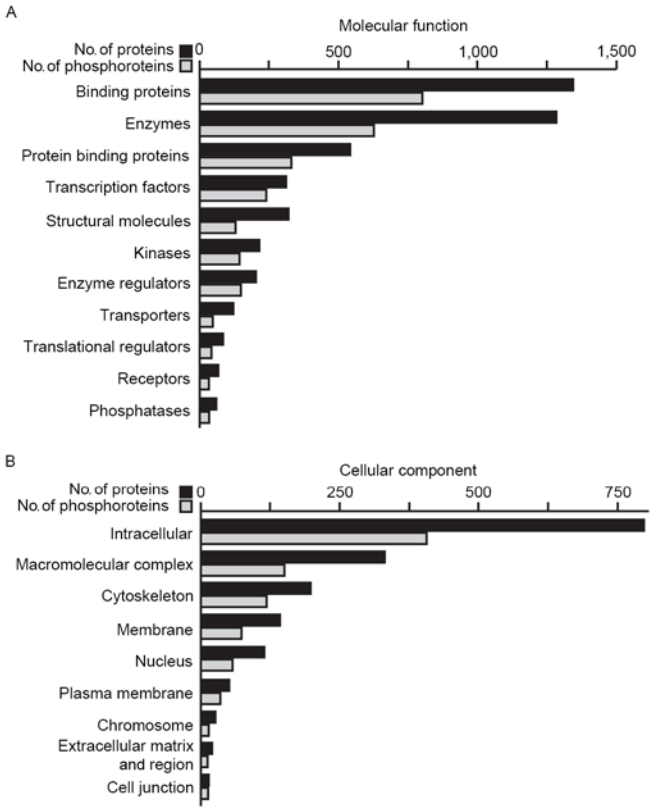

Figure 2. Molecular function and cellular localization distribution of proteins and phosphoproteins identified in the current study. The numbers of identified phosphoproteins with (A) different molecular functions and (B) cellular locations were calculated based on the information obtained from the PANTHER classification system.

induces apoptosis in MDA-MB-231 cells (8) and inhibits activation of the NF-κB signaling pathway (9). Furthermore, it has been demonstrated that Rg3 exhibits different anticancer effects in different cancer cell lines (22-28). To identify other changes in the signaling network induced by Rg3 in breast cancer cells, TMT-based quantitative analysis of phosphoproteomic changes in MDA-MB-231 cells was performed following treatment with Rg3. Kim *et al* (9) suggested that Rg3 inhibits the phosphorylation of Akt and ERK following 24 h treatment in MDA-MB-231 cells. Therefore, the current study examined phosphoproteomic changes in MDA-MB-231 cells 3 and 24 h following Rg3 treatment. Cells were treated with Rg3 at the indicated times and harvested for TMT-labeling (Fig. 1). Labeled peptides from 6 samples were mixed, fractionated and subjected to LC-MS/MS analysis.

MS data generated through 18 LC-MS/MS runs were analyzed on the MaxQuant proteomics data analysis platform (Version 1.4.1.2) (18,29). Using an FDR cut-off of 1% at the peptide and protein levels and excluding reverse and contaminating matchers, 3,597 proteins were identified, of which 2,143 were phosphoproteins. From these phosphoproteins, a total of 5,907 phosphorylation sites were detected. Files describing the identification of these proteins and their phosphorylation sites may be downloaded from the PRIDE partner repository using the following link (http://www.ebi.ac.uk/pride/archive/projects/PXD003092/files). These files include information about sequence coverage information, protein/peptide identification score and peptide sequences. These proteins and phosphoproteins were categorized according to molecular function (Fig. 2A) or cellular component (Fig. 2B) using the PANTHER classification system.

Reporter ion intensities were calculated using MaxQuant to quantify changes in the expression and phosphorylation levels of these proteins. A total of 2,118 proteins and 5,140 phosphorylation sites on 2,041 phosphoproteins were quantified. In several proteomics studies that also used TMT-based quantitative methods, a 1.5 fold change was selected as the cut-off for significant changes (12,14,30). Therefore, a 1.5 fold-cutoff for increases and a 0.67 fold-cutoff for decreases at the protein and phosphorylation levels were selected in the current study. Observed changes that were consistent in the biological replicate experiments were considered to be reliable observations. Following the aforementioned criteria, changes in the expression and phosphorylation of proteins in ginsenoside Rg3-treated MDA-MB-231 cells was analyzed (Fig. 3). The results of the current study indicated that the expression of 2,117 quantified proteins in MDA-MB-231 cells remained unchanged following 3 and 24 h treatment with Rg3 (Fig. 3A

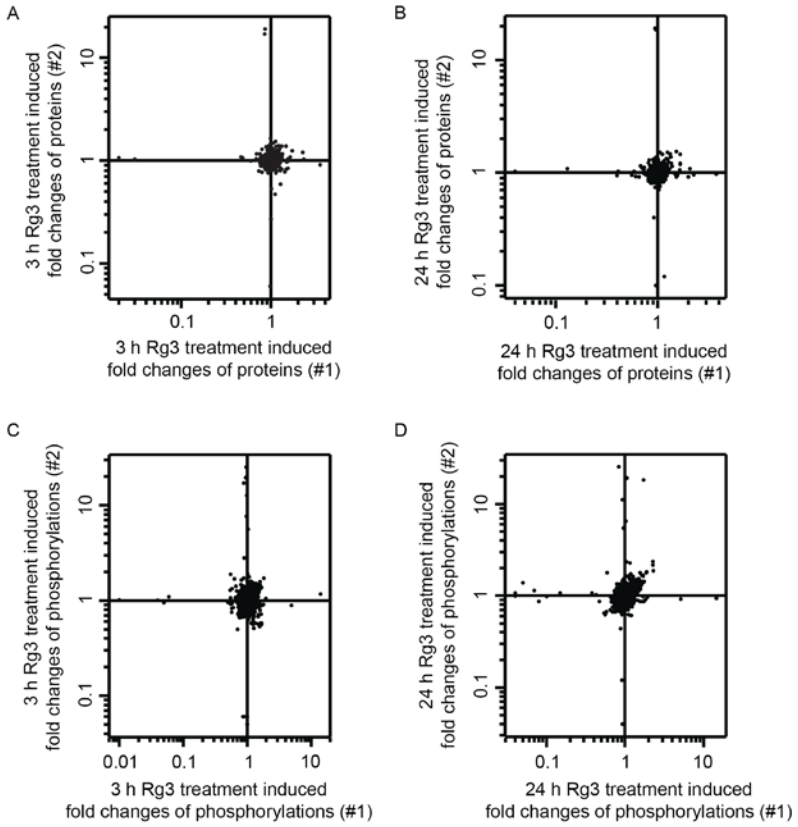

Figure 3. Quantitative analysis of fold changes of proteins and phosphorylation in ginsenoside Rg3-treated MDA-MB-231 cells. Density scatter plot of fold changes of (A and B) protein expression and (C and D) level of protein phosphorylation at (A and C) 3 h and (B and D) 24 h in ginsenoside Rg3-treated MDA-MB-231 cells. All the data have been log10-transformed.

and B) and that Rg3 increased the expression of one protein, 40S ribosomal protein S27 (Fig. 4), suggesting that Rg3 may have little effect on the total protein expression in MDA-MB-231 cells following 24 h treatment. Furthermore, the results of the present study demonstrated that the phosphorylation level on 5,127 quantified sites of 2,038 proteins in MDA-MB-231 cells remained unchanged following treatment for 3 and 24 h (Fig. 3C and D) and that Rg3 was able to regulate the phosphorylation level of 12 proteins on the 13 sites (Table I). Among these 12 Rg3-regulated phosphoproteins, the results demonstrated that the expression of 9 Rg3-regulated phosphoproteins remained unchanged. Furthermore, there were no quantitative data evaluating changes in the expression of HIRA-interacting protein 3 (HIRIP3), MYC binding protein 2 (MYCBP2) and PRKC apoptosis WT1 regulator protein (PAWR), suggesting that Rg3 changes the phosphorylation level of these proteins but does not affect their overall expression. Overall, 13 Rg3-regulated signaling molecules were identified in breast cancer cells.

Rg3-regulated signaling molecules in MDA-MB-231 cells. Rg3 affects various signaling pathways in cancer cells. To understand the potential impacts of these newly identified Rg3-regulated signaling molecules on the effects of Rg3 in MDA-MB-231 cells, a literature search was performed to review the functions of these signaling molecules identified in previous studies.

Ribosomal protein S27 (RPS27, previously known as metallopastimulin), a multifunctional protein, is a component of the ribosome 40S subunit and belongs to the S27E family of ribosomal proteins. RPS27 is highly expressed in a wide variety of malignant tumor tissues (31-36). RPS27 knockdown induces spontaneous apoptosis and inhibits the proliferation of human gastric cancer cells by inhibiting NF-κB signaling (37,38). However, the ectopic expression of RPS27 may also inhibit cell proliferation in head and neck squamous cell carcinoma cells (39). To the best of our knowledge, the current study is the first to indicate that RPS27 expression is increased in MDA-MB-231 cells following 24 h treatment with Rg3. Interestingly, the results of the current study did not identify increased phosphorylation at the Ser11 and Ser27 sites of RPS27 (Fig. 4B), suggesting that phosphorylation of RPS27 may not serve a role in the anti-proliferative role of Rg3 in MDA-MB-231 cells.

Cleavage and polyadenylation specificity factor subunit 7 (CPSF7) is a subunit of CPSF, which is responsible for the splicing and processing of the 3'-end during mRNA maturation (40,41). It has been demonstrated that the expression of *CPSF7* mRNA in cancer stroma is associated with the recurrence of breast cancer (42). In the current study, Rg-induced phosphorylation on CPSF7 was observed in MDA-MB-231 cells, indicating that CPSF7 may be involved in the development of breast cancer (Fig. 5A and Table I).

Myosin phosphatase is critical in the regulation of myosin light chain phosphorylation (43,44). Myosin light chain phosphorylation serves a critical role in the contraction of smooth muscles, as well as during cell division and cell migration (45).

Table I. A list of Rg3-regulated phosphoproteins.

Gene symbol	Protein	Uniprot ID	Phosphosite	Identified peptides	Fold change	
					3-h	24-h
CPSF7	Cleavage and polyadenylation specificity factor subunit 7	Q8N684	S191	AHpSRDSSDSADGR	1.52	2.08
EEF2	Elongation factor 2	P13639	T57	AGETRFpTDTR	1.78	2.21
HIRIP3	HIRA-interacting protein 3	Q9BW71	S372	EVSDpSEAGGGPQGER	0.72	0.60
MAGED2	Melanoma-associated antigen D2	Q9UNF1	S173	HLDGEEDGpSpSDQSQASGTTGGR	0.92	0.63
MPRIP	Myosin phosphatase Rho-interacting protein	Q6WCQ1	S218	TKDQPDGSpSLpSPAQSPS	1.58	1.21
			S220	QSQPPAASSLR	1.58	1.21
MYCBP2	Probable E3 ubiquitin-protein ligase MYCBP2	O75592	S2751	SLpSPNHNTLQTLK	1.11	1.52
PAWR	PRKC apoptosis WT1 regulator protein	Q96IZ0	S231	STTpSVSEEDVSSR	1.38	1.82
PPP1R12A	Protein phosphatase 1 regulatory subunit 12A	O14974	S695	RpSTQGVTLTDLQEAEK	1.44	2.32
RANBP2	E3 SUMO-protein ligase RanBP2	P49792	S1456	SGSSFVHQApSFK	1.19	1.85
SEPT9	Septin-9	Q9UHD8	S85	HVDSLSQRpSPK	1.39	1.68
TMPO	Thymopoietin	P42167	S156	EQGTEpSR	1.00	1.65
UFL1	E3 UFM1-protein ligase 1	O94874	S458	KDDDpSDDESQSSHTGK	1.18	1.66

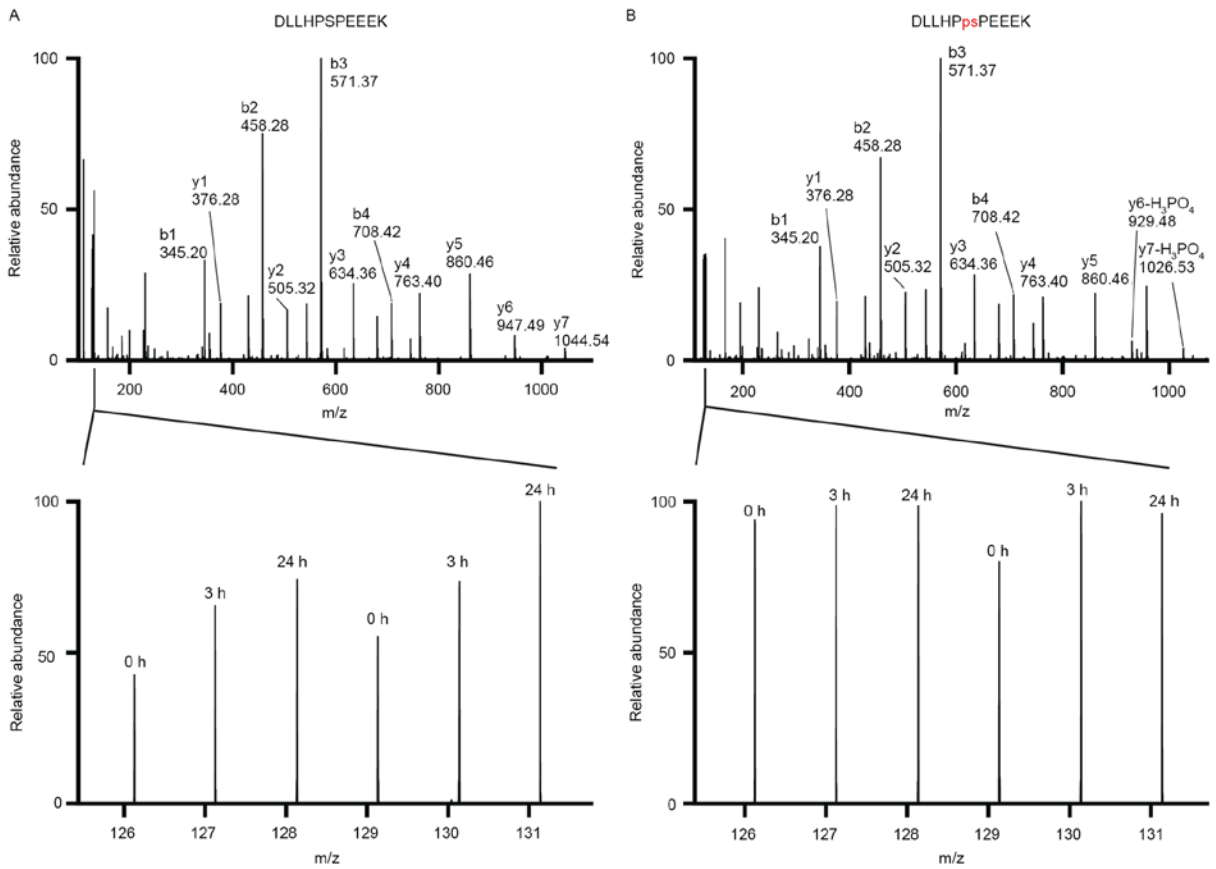

Figure 4. Ginsenoside Rg3 increases the expression of ribosomal protein S27 but does not affect its phosphorylation. (A) The MS/MS spectrum of the peptide DLLHPSPEEEK is annotated (above) and the relative intensities of the TMT reporter ions present the changes in its expression (below) in biological duplicates. (B) The MS/MS spectrum of the phosphopeptide DLLHPpSPEEEK is annotated (above) and the relative intensities of the TMT reporter ions present the unchanged phosphorylation level of RPS27 at Ser 11 (bottom). TMT, tandem mass tag; MS, mass spectrometry.

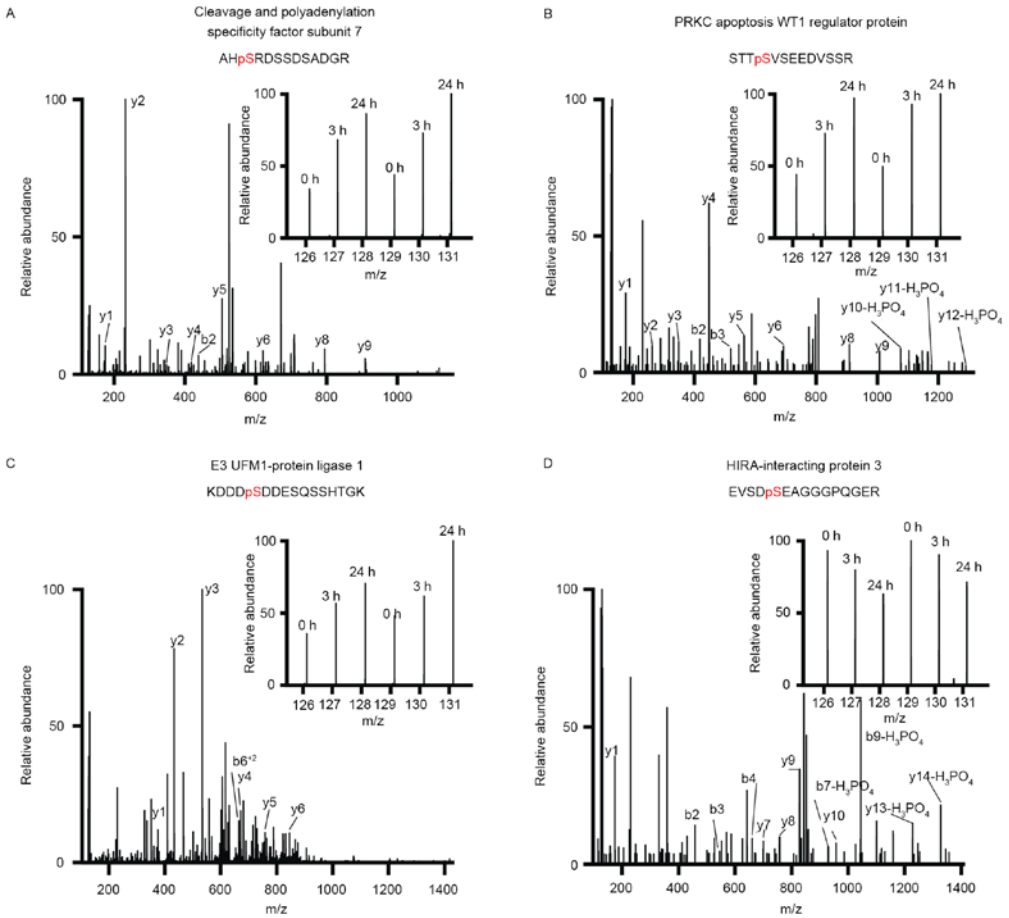

Figure 5. Representative MS/MS spectra of the identified phosphopeptides from (A) cleavage and polyadenylation specificity factor subunit 7, (B) HIRA-interacting protein 3, (C) potassium/sodium PRKC apoptosis WT1 regulator protein, and (D) E3 UFM1-protein ligase 1. Inset shows the relative intensities of the tandem mass tag reporter tags of ginsenoside Rg3 treatment at different time points. MS, mass spectrometry.

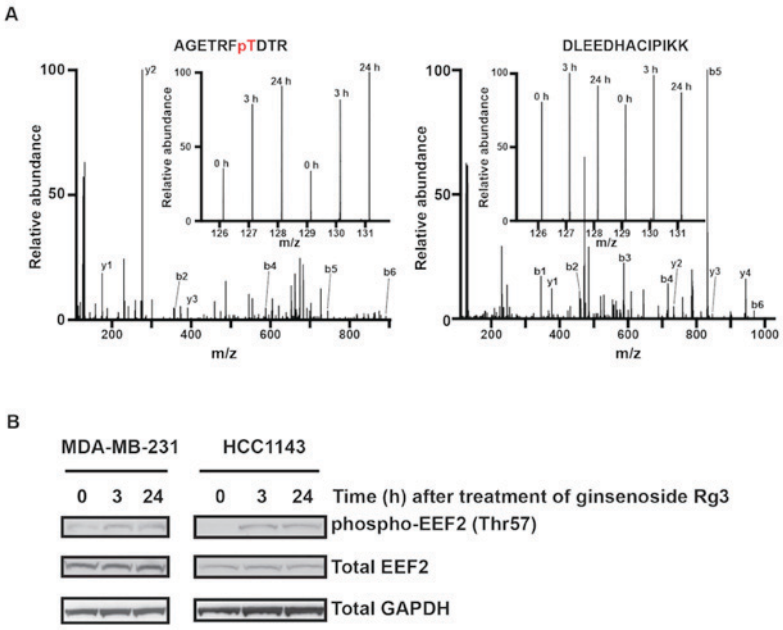

Figure 6. Ginsenoside Rg3 increases the phosphorylation level of EEF2 on Thr57. (A) Representative MS/MS spectra of the identified phosphopeptide AGETRFpTDTR (left) and the non-phosphopeptide DLEEDHACIPIKK (right) from EEF2. Inset presents the relative intensities of the TMT reporter tags following treatment with Rg3 at different time points in biological duplicates. (B) Time course of Rg3-induced EEF2 phosphorylation in MDA-MB-231 and HCC1143 cells. Following treatment with Rg3 for the indicated times, cells were subjected to lysis and resolved by SDS-PAGE. Threonine phosphorylation of EEF2 was probed by Western blotting with antibodies against phospho-EEF2 (Thr57). The amount of total EEF2 was determined by Western blotting with anti-EEF2 antibodies. The amount of total GAPDH was determined by Western blotting with antibodies against GAPDH as the loading control. TMT, tandem mass tag; EEF2, elongation factor 2; MS, mass spectrum; phospho, phosphorylated.

Two components of the myosin phosphatase complex, myosin phosphatase Rho-interacting protein (MPRIP) and myosin phosphatase target subunit 1 (PPP1R12A), were identified in the current study. MPRIP regulates myosin light chain phosphorylation and maintains actin stress fibers (46,47) whereas PPP1R12A serves roles in various actin-involved biological processes, including chromatid segregation (48) and cell migration (49). The results of the current study demonstrated that Rg3 increased phosphorylation on MPRIP and PPP1R12A. Septin-9 (SEPT9) belongs to a family of guanosine triphosphate (GTP)-binding proteins, septins that have been implicated in mammalian cell division. SEPT9 is critical for the final separation of daughter cells but is not required during the early stages of cell division (50). This gene is the only gene in which mutations are known to cause hereditary neuralgic amyotrophy (51). The results of the current study indicate that the phosphorylation of SEPT-9 is increased following treatment with Rg3 in MDA-MB-231 cells. Taken together, these results indicate that Rg3 may serve a role in regulating cell division.

MYCBP2, also known as PAM, is known as one of the most potent inhibitors of adenylyl cyclase and mediates the inhibition of cyclic adenosine monophosphate signaling (52). PAWR is well known by the name of prostate apoptosis response-4 (Par-4) due to its unique ability to induce apoptosis in cancer cells but not in healthy cells (53). RANBP2 is a giant scaffold and mosaic cyclophilin-related nucleoporin and has been implicated in transportin-dependent nuclear import (54,55). The results of the current study indicated that Rg3 treatment increased the phosphorylation of these three proteins (Fig. 5B and Table I).

E3 ubiquitin fold modifier 1 (UFM1)-protein ligase 1 (UFL1) is a ligase specifically responsible for the UFM1, a ubiquitin-like modifier covalently conjugated to its target proteins (56). UFL1-mediated UFM1 modification serves an important role in various signaling pathways, including inhibition of NF-κB signaling (57) and regulation of the cell cycle (58). It has been demonstrated that Rg inhibits NF-κB signaling in various types of human cancer (9,59,60). The results of the current study indicate that Rg3 may increase the phosphorylation of UFL1 in MDA-MB-231 cells (Fig. 5C and Table I), suggesting that Rg3 may inhibit NF-κB signaling by regulating UFL1-mediated UFM1 modification.

Rg3 also decreased the phosphorylation of HIRIP3 and MGED2 (Fig. 5D and Table I). HIRIP3 is an interacting protein of the HIRA protein, a histone chaperon and its function remains largely unknown (61). MGED2 is a potential negative regulator of p53, a tumor suppressor gene (62) and may protect against tumor necrosis factor-related apoptosis-inducing ligand (TRAIL)-induced apoptosis in human melanoma cells (63).

Elongation factor 2 (EEF2) is a member of the GTP-binding translation elongation factor family and is an essential factor for protein synthesis. Phosphorylation of EEF2 on Thr57 impairs protein synthesis (64,65). As presented in Fig. 6A, Rg3 increases the phosphorylation of EEF2 on the Thr57 site (Table I), suggesting that Rg3 may suppress protein synthesis in MDA-MB-231 cells.

The majority of Rg3-regulated phosphorylation events have not been previously investigated. Among the 13 phosphorylation sites listed in Table I, only phosphorylation-specific antibodies against pThr57 of EEF2 is commercially available. Western blotting was performed to determine whether the expression of EEF2 and p-EEF2 were altered by Rg3 in MDA-MB-231 and HCC1143 TNBC cells. The results demonstrated that Rg3 increased the phosphorylation of EEF2 on Thr57 but did not affect the total expression of EEF2 in MDA-MB-231 and HCC1143 cells (Fig. 6B). These results were consistent with those of quantitative phosphoproteomics, validating these results.

In conclusion, the results of the current study demonstrated that during short term treatment with Rg3, MDA-MB-231 cells were not dramatically altered at the proteomic level. Rg3-induced changes in the phosphorylation of proteins involved in protein synthesis, cell division and inhibition of NF-κB signaling were detected. The present study suggests that Rg3 exerts its effects on cellular proliferation in diverse ways; however, further studies are required to improve understanding of the anticancer effects of Rg3.

Acknowledgements

The present study was supported by the Fundamental Research Funds for the Cancer Hospital, Chinese Academy of Medical Sciences (grant no. JK2014B10), the National Natural Science Foundation of China (grant no. 81372829), Beijing Municipal Natural Science Foundation (grant no. 7142140), and Shandong Province Science and Technology Development Program (grant no. 2010GSF 10283).

References

1. Chen W, Zheng R, Zeng H, Zhang S and He J: Annual report on status of cancer in China, 2011. Chin J Cancer Res 27: 2-12, 2015.
2. Song QK, Wang XL, Zhou XN, Yang HB, Li YC, Wu JP, Ren J and Lyerly HK: Breast cancer challenges and screening in China: Lessons from current registry data and population screening studies. Oncologist 20: 773-779, 2015.
3. Ma R, Sun L, Chen X, Mei B, Chang G, Wang M and Zhao D: Proteomic analyses provide novel insights into plant growth and ginsenoside biosynthesis in forest cultivated *panax ginseng* (F. Ginseng). Front Plant Sci 7: 1, 2016.
4. Colzani M, Altomare A, Caliendo M, Aldini G, Righetti PG and Fasoli E: The secrets of Oriental panacea: *Panax ginseng*. J Proteomics 130: 150-159, 2016.
5. Xie G, Wang CZ, Yu C, Qiu Y, Wen XD, Zhang CF, Yuan CS and Jia W: Metabonomic profiling reveals cancer chemopreventive effects of american ginseng on colon carcinogenesis in Apc (Min/+) mice. J Proteome Res 14: 3336-3347, 2015.
6. Gillis CN: *Panax ginseng* pharmacology: A nitric oxide link? Biochem Pharmacol 54: 1-8, 1997.
7. Chen XP, Qian LL, Jiang H and Chen JH: Ginsenoside Rg3 inhibits CXCR4 expression and related migrations in a breast cancer cell line. Int J Clin Oncol 16: 519-523, 2011.
8. Kim BM, Kim DH, Park JH, Na HK and Surh YJ: Ginsenoside Rg3 induces apoptosis of human breast cancer (MDA-MB-231) cells. J Cancer Prev 18: 177-185, 2013.
9. Kim BM, Kim DH, Park JH, Surh YJ and Na HK: Ginsenoside Rg3 inhibits constitutive activation of NF-κB signaling in human breast cancer (MDA-MB-231) cells: ERK and Akt as potential upstream targe. J Cancer Prev 19: 23-30, 2014.
10. Thompson A, Schäfer J, Kuhn K, Kienle S, Schwarz J, Schmidt G, Neumann T, Johnstone R, Mohammed AK and Hamon C: Tandem mass tags: A novel quantification strategy for comparative analysis of complex protein mixtures by MS/MS. Anal Chem 75: 1895-1904, 2003.
11. Ross PL, Huang YN, Marchese JN, Williamson B, Parker K, Hattan S, Khainovski N, Pillai S, Dey S, Daniels S, *et al*: Multiplexed protein quantitation in Saccharomyces cerevisiae using amine-reactive isobaric tagging reagents. Mol Cell Proteomics 3: 1154-1169, 2004.

12. Nirujogi RS, Wright JD Jr, Manda SS, Zhong J, Na CH, Meyerhoff J, Benton B, Jabbour R, Willis K, Kim MS, *et al*: Phosphoproteomic analysis reveals compensatory effects in the piriform cortex of VX nerve agent exposed rats. Proteomics 15: 487-499, 2015.
13. Roitinger E, Hofer M, Kocher T, Pichler P, Novatchkova M, Yang J, Schlögelhofer P and Mechtler K: Quantitative phosphoproteomics of the ataxia telangiectasia-mutated (ATM) and ataxia telangiectasia-mutated and rad3-related (ATR) dependent DNA damage response in *Arabidopsis thaliana*. Mol Cell Proteomics 14: 556-571, 2015.
14. Fang Y, Zhang Q, Wang X, Yang X, Wang X, Huang Z, Jiao Y and Wang J: Quantitative phosphoproteomics reveals genistein as a modulator of cell cycle and DNA damage response pathways in triple-negative breast cancer cells. Int J Oncol 48: 1016-1028, 2016.
15. Wisniewski JR, Zougman A, Nagaraj N and Mann M: Universal sample preparation method for proteome analysis. Nat Methods 6: 359-362, 2009.
16. Larsen MR, Thingholm TE, Jensen ON, Roepstorff P and Jørgensen TJ: Highly selective enrichment of phosphorylated peptides from peptide mixtures using titanium dioxide microcolumns. Mol Cell Proteomics 4: 873-886, 2005.
17. Rappsilber J, Ishihama Y and Mann M: Stop and go extraction tips for matrix-assisted laser desorption/ionization, nanoelectrospray, and LC/MS sample pretreatment in proteomics. Anal Chem 75: 663-670, 2003.
18. Cox J and Mann M: MaxQuant enables high peptide identification rates, individualized p.p.b.-range mass accuracies and proteome-wide protein quantification. Nat Biotechnol 26: 1367-1372, 2008.
19. Vizcaino JA, Deutsch EW, Wang R, Csordas A, Reisinger F, Rios D, Dianes JA, Sun Z, Farrah T, Bandeira N, *et al*: ProteomeXchange provides globally coordinated proteomics data submission and dissemination. Nat Biotechnol 32: 223-226, 2014.
20. Mi H, Muruganujan A and Thomas PD: PANTHER in 2013: modeling the evolution of gene function, and other gene attributes, in the context of phylogenetic trees. Nucleic Acids Res 41 (Database issue): D377-D386, 2013.
21. Mi H, Muruganujan A, Casagrande JT and Thomas PD: Large-scale gene function analysis with the PANTHER classification system. Nat Protoc 8: 1551-1566, 2013.
22. Shan X, Aziz F, Tian LL, Wang XQ, Yan Q and Liu JW: Ginsenoside Rg3-induced EGFR/MAPK pathway deactivation inhibits melanoma cell proliferation by decreasing FUT4/LeY expression. Int J Oncol 46: 1667-1676, 2015.
23. Wang JH, Nao JF, Zhang M and He P: 20(s)-ginsenoside Rg3 promotes apoptosis in human ovarian cancer HO-8910 cells through PI3K/Akt and XIAP pathways. Tumour Biol 35: 11985-11994, 2014.
24. Shan X, Fu YS, Aziz F, Wang XQ, Yan Q and Liu JW: Ginsenoside Rg3 inhibits melanoma cell proliferation through down-regulation of histone deacetylase 3 (HDAC3) and increase of p53 acetylation. PLoS One 9: e115401, 2014.
25. Liu T, Zhao L, Zhang Y, Chen W, Liu D, Hou H, Ding L and Li X: Ginsenoside 20(S)-Rg3 targets HIF-1α to block hypoxia-induced epithelial-mesenchymal transition in ovarian cancer cells. PLoS One 9: e103887, 2014.
26. Kim BJ, Nah SY, Jeon JH, So I and Kim SJ: Transient receptor potential melastatin 7 channels are involved in ginsenoside Rg3-induced apoptosis in gastric cancer cells. Basic Clin Pharmacol Toxicol 109: 233-239, 2011.
27. Lee SY, Kim GT, Roh SH, Song JS, Kim HJ, Hong SS, Kwon SW and Park JH: Proteomic analysis of the anti-cancer effect of 20S-ginsenoside Rg3 in human colon cancer cell lines. Biosci Biotechnol Biochem 73: 811-816, 2009.
28. Luo Y, Zhang P, Zeng HQ, Lou SF and Wang DX: Ginsenoside Rg3 induces apoptosis in human multiple myeloma cells via the activation of Bcl-2-associated X protein. Mol Med Rep 12: 3557-3562, 2015.
29. Cox J, Matic I, Hilger M, Nagaraj N, Selbach M, Olsen JV and Mann M: A practical guide to the MaxQuant computational platform for SILAC-based quantitative proteomics. Nat Protoc 4: 698-705, 2009.
30. Wang Z, Liang S, Lian X, Liu L, Zhao S, Xuan Q, Guo L, Liu H, Yang Y, Dong T, *et al*: Identification of proteins responsible for adriamycin resistance in breast cancer cells using proteomics analysis. Sci Rep 5: 9301, 2015.
31. Fernandez-Pol JA: Increased serum level of RPMPS-1/S27 protein in patients with various types of cancer is useful for the early detection, prevention and therapy. Cancer Genomics Proteomics 9: 203-256, 2012.
32. Stack BC Jr, Dalsaso TA, Lee C Jr, Lowe VJ, Hamilton PD, Fletcher JW and Fernandez-Pol JA: Overexpression of MPS antigens by squamous cell carcinomas of the head and neck: Immunohistochemical and serological correlation with FDG positron emission tomography. Anticancer Res 19: 5503-5510, 1999.
33. Ganger DR, Hamilton PD, Klos DJ, Jakate S, McChesney L and Fernandez-Pol JA: Differential expression of metallopanstimulin/S27 ribosomal protein in hepatic regeneration and neoplasia. Cancer Detect Prev 25: 231-236, 2001.
34. Santa Cruz DJ, Hamilton PD, Klos DJ and Fernandez-Pol JA: Differential expression of metallopanstimulin/S27 ribosomal protein in melanocytic lesions of the skin. J Cutan Pathol 24: 533-542, 1997.
35. Ganger DR, Hamilton PD, Fletcher JW and Fernandez-Pol JA: Metallopanstimulin is overexpressed in a patient with colonic carcinoma. Anticancer Res 17: 1993-1999, 1997.
36. Fernandez-Pol JA, Fletcher JW, Hamilton PD and Klos DJ: Expression of metallopanstimulin and oncogenesis in human prostatic carcinoma. Anticancer Res 17: 1519-1530, 1997.
37. Yang ZY, Qu Y, Zhang Q, Wei M, Liu CX, Chen XH, Yan M, Zhu ZG, Liu BY, Chen GQ, *et al*: Knockdown of metallopanstimulin-1 inhibits NF-κB signaling at different levels: The role of apoptosis induction of gastric cancer cells. Int J Cancer 130: 2761-2770, 2012.
38. Wang YW, Qu Y, Li JF, Chen XH, Liu BY, Gu QL and Zhu ZG: In vitro and in vivo evidence of metallopanstimulin-1 in gastric cancer progression and tumorigenicity. Clin Cancer Res 12: 4965-4973, 2006.
39. Dai Y, Pierson SE, Dudney WC and Stack BC Jr: Extraribosomal function of metallopanstimulin-1: Reducing paxillin in head and neck squamous cell carcinoma and inhibiting tumor growth. Int J Cancer 126: 611-619, 2010.
40. Kim S, Yamamoto J, Chen Y, Aida M, Wada T, Handa H and Yamaguchi Y: Evidence that cleavage factor Im is a heterotetrameric protein complex controlling alternative polyadenylation. Genes Cells 15: 1003-1013, 2010.
41. Millevoi S, Loulergue C, Dettwiler S, Karaa SZ, Keller W, Antoniou M and Vagner S: An interaction between U2AF 65 and CF I(m) links the splicing and 3' end processing machineries. EMBO J 25: 4854-4864, 2006.
42. Verghese ET, Drury R, Green CA, Holliday DL, Lu X, Nash C, Speirs V, Thorne JL, Thygesen HH, Zougman A, *et al*: MiR-26b is down-regulated in carcinoma-associated fibroblasts from ER-positive breast cancers leading to enhanced cell migration and invasion. J Pathol 231: 388-399, 2013.
43. Trinkle-Mulcahy L and Lamond AI: Mitotic phosphatases: No longer silent partners. Curr Opin Cell Biol 18: 623-631, 2006.
44. Ito M, Nakano T, Erdodi F and Hartshorne DJ: Myosin phosphatase: Structure, regulation and function. Mol Cell Biochem 259: 197-209, 2004.
45. Matsumura F and Hartshorne DJ: Myosin phosphatase target subunit: Many roles in cell function. Biochem Biophys Res Commun 369: 149-156, 2008.
46. Vallenius T, Vaahtomeri K, Kovac B, Osiceanu AM, Viljanen M and Mäkelä TP: An association between NUAK2 and MRIP reveals a novel mechanism for regulation of actin stress fibers. J Cell Sci 124: 384-393, 2011.
47. Surks HK, Riddick N and Ohtani K: M-RIP targets myosin phosphatase to stress fibers to regulate myosin light chain phosphorylation in vascular smooth muscle cells. J Biol Chem 280: 42543-42551, 2005.
48. Matsumura F, Yamakita Y and Yamashiro S: Myosin phosphatase-targeting subunit 1 controls chromatid segregation. J Biol Chem 286: 10825-10833, 2011.
49. Xia D, Stull JT and Kamm KE: Myosin phosphatase targeting subunit 1 affects cell migration by regulating myosin phosphorylation and actin assembly. Exp Cell Res 304: 506-517, 2005.
50. Estey MP, Di Ciano-Oliveira C, Froese CD, Bejide MT and Trimble WS: Distinct roles of septins in cytokinesis: SEPT9 mediates midbody abscission. J Cell Biol 191: 741-749, 2010.
51. van Alfen N, Hannibal MC, Chance PF and van Engelen BGM: Hereditary neuralgic amyotrophy. in: Pagon RA, Adam MP, Ardinger HH, Wallace SE, Amemiya A, Bean LJH, Bird TD, Fong CT, Smith RJH, Stephens K (Eds). GeneReviews (R), Seattle (WA): University of Washington, 1993.
52. Pierre SC, Häusler J, Birod K, Geisslinger G and Scholich K: PAM mediates sustained inhibition of cAMP signaling by sphingosine-1-phosphate. EMBO J 23: 3031-3040, 2004.

53. Hebbar N, Shrestha-Bhattarai T and Rangnekar VM: Cancer-selective apoptosis by tumor suppressor par-4. Adv Exp Med Biol 818: 155-166, 2014.
54. Hutten S, Walde S, Spillner C, Hauber J and Kehlenbach RH: The nuclear pore component Nup358 promotes transportin-dependent nuclear import. J Cell Sci 122: 1100-1110, 2009.
55. Wälde S, Thakar K, Hutten S, Spillner C, Nath A, Rothbauer U, Wiemann S and Kehlenbach RH: The nucleoporin Nup358/RanBP2 promotes nuclear import in a cargo- and transport receptor-specific manner. Traffic 13: 218-233, 2012.
56. Tatsumi K, Sou YS, Tada N, Nakamura E, Iemura S, Natsume T, Kang SH, Chung CH, Kasahara M, Kominami E, *et al*: A novel type of E3 ligase for the Ufm1 conjugation system. J Biol Chem 285: 5417-5427, 2010.
57. Wu J, Lei G, Mei M, Tang Y and Li H: A novel C53/LZAP-interacting protein regulates stability of C53/LZAP and DDRGK domain-containing Protein 1 (DDRGK1) and modulates NF-kappaB signaling. J Biol Chem 285: 15126-15136, 2010.
58. Kim CH, Nam HS, Lee EH, Han SH, Cho HJ, Chung HJ, Lee NS, Choi SJ, Kim H, Ryu JS, *et al*: Overexpression of a novel regulator of p120 catenin, NLBP, promotes lung adenocarcinoma proliferation. Cell Cycle 12: 2443-2453, 2013.
59. Wang L, Li X, Song YM, Wang B, Zhang FR, Yang R, Wang HQ and Zhang GJ: Ginsenoside Rg3 sensitizes human non-small cell lung cancer cells to γ-radiation by targeting the nuclear factor-κB pathway. Mol Med Rep 12: 609-614, 2015.
60. Kim SM, Lee SY, Cho JS, Son SM, Choi SS, Yun YP, Yoo HS, Yoon DY, Oh KW, Han SB and Hong JT: Combination of ginsenoside Rg3 with docetaxel enhances the susceptibility of prostate cancer cells via inhibition of NF-kappaB. Eur J Pharmacol 631: 1-9, 2010.
61. Lorain S, Quivy JP, Monier-Gavelle F, Scamps C, Lécluse Y, Almouzni G and Lipinski M: Core histones and HIRIP3, a novel histone-binding protein, directly interact with WD repeat protein HIRA. Mol Cell Biol 18: 5546-5556, 1998.
62. Papageorgio C, Brachmann R, Zeng J, Culverhouse R, Zhang W and McLeod H: MAGED2: A novel p53-dissociator. Int J Oncol 31: 1205-1211, 2007.
63. Tseng HY, Chen LH, Ye Y, Tay KH, Jiang CC, Guo ST, Jin L, Hersey P and Zhang XD: The melanoma-associated antigen MAGE-D2 suppresses TRAIL receptor 2 and protects against TRAIL-induced apoptosis in human melanoma cells. Carcinogenesis 33: 1871-1881, 2012.
64. Redpath NT, Price NT, Severinov KV and Proud CG: Regulation of elongation factor-2 by multisite phosphorylation. Eur J Biochem 213: 689-699, 1993.
65. Horman S, Browne G, Krause U, Patel J, Vertommen D, Bertrand L, Lavoinne A, Hue L, Proud C and Rider M: Activation of AMP-activated protein kinase leads to the phosphorylation of elongation factor 2 and an inhibition of protein synthesis. Curr Biol 12: 1419-1423, 2002.